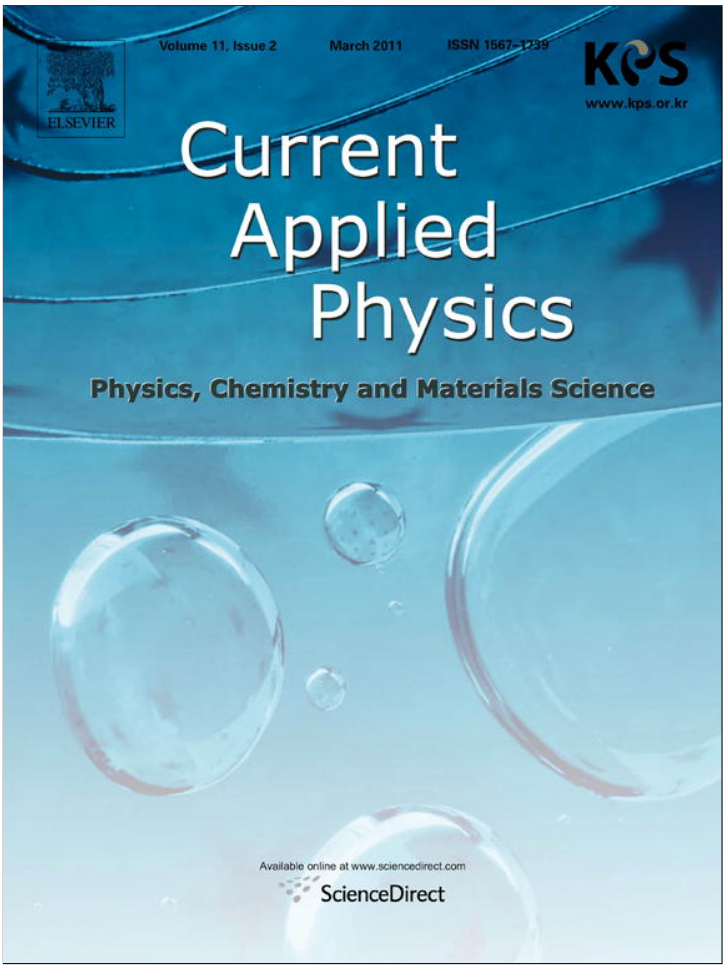

Current Applied Physics 10 (2010) e118–e121

Contents lists available at ScienceDirect

Current Applied Physics

journal homepage: www.elsevier.com/locate/cap

# Measurement of local retardation in optically isotropic liquid crystal devices driven by in-plane electric field

Miyoung Kim [a,b], Byeong Gyun Kang [c], Min Su Kim [b], Mi-Kyung Kim [b], Pankaj Kumar [b], Myong-Hoon Lee [b], Shin-Woong Kang [c,*], Seung Hee Lee [b,c,*]

[a] Korea Electronics Technology Institute Palbokdong 2-ga, Deokjin-gu, Jeonju, Chonbuk 561-844, Republic of Korea
[b] Polymer Fusion Research Center, Department of Polymer-Nano Science and Technology, Chonbuk National University, 1Ga 664-14, Deokjin-dong, Deokjin-ku, Jeonju, Jeonbuk 561-756, Republic of Korea
[c] Department of BIN Fusion Technology, Chonbuk National University, Jeonju, Jeonbuk 561-756, Republic of Korea

ARTICLE INFO

*Article history:*
Received 3 January 2010
Received in revised form
8 April 2010
Accepted 10 June 2010
Available online 25 June 2010

*Keywords:*
Liquid crystals
Optical retardation
Blue phase
Kerr effect

ABSTRACT

The novel method to measure a local optical retardation has been proposed. By combining an *electrically controllable birefringence* (ECB) liquid crystal (LC) cell and image processing software, the local retardation of a polymer-stabilized blue phase (BP) with in-plane electric field has successfully been measured in a micrometer scale. When the optic axes of the sample and reference cells are aligned ±45° with respect to the crossed polarizers, the optical retardation of the sample is compensated by a reference ECB cell. In this geometry, the optical retardation or birefringence of micro-domains can be experimentally quantified by determining a complete compensation condition with electrically adjustable reference cell and image processing software. This method is very useful to measure Kerr constant of the BPLC more exactly and also can be applied for various samples that require a micrometer scale resolution for the measurement of optical retardation.



## 1. Introduction

The nematic liquid crystals (LCs) with different operating modes such as twisted nematic (TN), super twisted nematic (STN), in-plane switching (IPS), fringe-field switching (FFS) and multi-domain vertical alignment (MVA) have been utilized as a major LC component in the field of liquid crystal display technology [1–4]. Polymer stabilization of various LC phases has also been widely investigated over the last two decades [5–7]. In recent years, the polymer stabilizations of cholesteric blue phases (PSBPs) and nano-structured cholesteric LCs have been attracting a great deal of attentions due to their promising properties such as fast response time, ideal dark state, and no need of surface treatment, etc. Especially, their optical isotropy with a local liquid crystalline order renders an extraordinarily large *Kerr constant* and thus the fast transition from the optically isotropic to birefringent state by applying external electric field. [8–14].

In the optically isotropic LC state, a field-off state under crossed polarizers is completely dark (i.e., ideal off-state) according to the isotropic organizations of LC domains. In the existence of an electric field within a practical range, the optical birefringence is induced due to its intrinsic liquid crystalline order and its magnitude is determined by the Eq. (1).

$$\Delta n_i = \lambda K E^2 \tag{1}$$

where $\Delta n_i$ is the induced birefringence, $\lambda$ is the wavelength of the incident light, $K$ is the *Kerr constant* of the LC mixture and $E$ is the applied electric field [9–15]. The optical transmittance associated with the induced phase retardation under crossed polarizers can be described as follows:

$$T/T_0 = \sin^2 2\psi(V) \sin^2(\pi d \Delta n_i(V)/\lambda) \tag{2}$$

where $\psi(V)$ is the voltage dependent angle between a uniaxial optic axis of LC and one of the transmission axes of crossed polarizers in the plane of substrate, $d$ is the thickness of LC layer, and $\Delta n_i(V)$ is the induced birefringence as a function of applied voltage. For the maximum transmittance, $\psi$ and $d\Delta n_i$ should be equal to 45° and $\lambda/2$, respectively [16].

The optically isotropic LC cells can be stabilized by internal polymer networks and hence significantly extend their operating temperature range [8]. When they are operated by the in-plane electric field with interdigitated electrodes, the induced optical retardation in a pixel area (i.e., area between electrodes) is not uniform, resulting in a gradient of optical transmittance. To

* Corresponding authors. Department of BIN Fusion Technology, Chonbuk National University, Jeonju, Jeonbuk 561-756, Republic of Korea. Tel.: +82 63 270 2343; fax: +82 63 270 2341.
*E-mail addresses:* swkang@jbnu.ac.kr (S.-W. Kang), lsh1@chonbuk.ac.kr (S.H. Lee).

1567-1739/$ – see front matter © 2010 Elsevier B.V. All rights reserved.
doi:10.1016/j.cap.2010.06.012

optimize a brightness of pixel area and maximize device performance, it is necessary to measure local retardations caused by nonuniform electric field in between electrode.

In this paper, we report the measurement method of a local retardation of LC devices by using an *electrically controllable birefringence* (ECB) cell. The retardation value of the ECB cell can be controlled by an applying electric field and used as a reference to measure a local retardation of the sample as a function of applied field. To demonstrate this concept, we employed a *Kerr cell* (i.e., *polymer-stabilized blue phase*) with an in-plane electric field as a test sample and investigated a local retardation in a micrometer scale. The optical transmittance was recorded under a polarizing optical microscope (POM) to determine a complete optical compensation between sample and reference cells and the POM images were analyzed using image processing software. The local retardation values were measured by the reference cell at a complete compensation condition.

## 2. Experiments

*Preparation of electro-optic cells*: In this experiment, we fabricated IPS type of electro-optic cells [17]. The bottom substrate consisted of pixel electrodes with patterned indium-tin-oxide (ITO) and common electrodes with patterned Mo–Ti alloy on a flat glass. The width and separation of patterned-electrodes with a wedge shape were 10 μm and 20 μm, respectively. The 10 μm-thick adhesive tape was used to maintain a gap between top and bottom substrates. The measured gap of empty cells prior to LC load was $10 \pm 0.1$ μm. The dimension of cells used in the experiments was 3.0 cm × 2.7 cm with an active area of 1.5 cm × 1.5 cm.

*Preparation of LC mixture*: Our sample was a mixture of the nematic liquid crystal, chiral additives, reactive monomers, and a photoinitiator (Irgacure 651, Ciba Additive Corp.). The nematic LC used in this study was a cyano-biphenyl type mixture purchased from Merck. We used two reactive monomers, nonmesogenic ethylhexyl acrylate EHA (Aldrich) and the nematic mesogen RM257 (Merck). The chiral additives ZLI 4572 and CB 15 both purchased from Merck were used to adjust a helical pitch of the LC mixture. The sample components were mixed by following weight ratio: nematic LC (33.0 wt%), ZLI 4572 (8.0 wt%), CB 15 (10.5 wt%), RM257 (46.0 wt%), EHA (1.9 wt%), and photoinitiator (0.6 wt%).

*Polymer stabilization*: The cholesteric mixture was then loaded into 10 μm-thick E.O. cells in the isotropic phase (100 °C). The sample cells were then cooled to 91 °C and annealed for ten minutes before polymer stabilization. For the polymer stabilization, the sample cells were exposed with UV-light generated by a Hg–Xe source L9588-01 (Hamamatsu) for two hours with an intensity of 5 mW/cm$^2$.

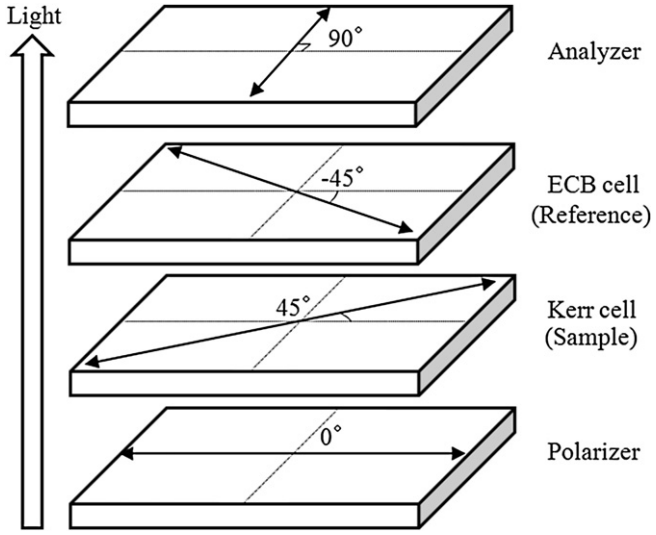


**Fig. 2.** Schematic illustration of the method to measure a local retardation of the *Kerr* cell. The in-plane optic axes of the *Kerr* (sample) and ECB (reference) cells are aligned +45° and −45° with respect to the transmission axis of a polarizer. The light normally enters the substrate plane from the bottom as indicated by a single-headed arrow.

*Preparation of a reference ECB cell*: The reference ECB cell was constructed using flat glass substrates with ITO layer. The inner surfaces were treated with antiparallel rubbed polyimide alignment layers with a low pretilt angle. The nematic LC with $\Delta n = 0.088$ was loaded into 4.0 μm thick cell. The variable retardations of the ECB cell were calibrated as a function of applied voltage by measuring retardation values at 550 nm using a REMS-150 (SESIM Photonics Technology).

*Polarizing optical microscopy (POM)*: For the microscopic textural study, the cells filled with a cholesteric mixture were placed under Nikon DXM1200 POM with crossed polarizers in a transmission mode. The micro-photographic images were recorded using POM.

*Simulation conditions*: For the calculation of electro-optic characteristics of a *Kerr* sample, we used commercial software "TechWiz LCD" (Sanayi System Corp.). The simulation parameters such as cell configuration, electrode dimension and material properties were the same as experimental conditions.

## 3. Results and discussion

The cholesteric mixture, polymer-stabilized at 91 °C in the blue phase, exhibited an optically isotropic state which is a dark under crossed polarizers as seen in Fig. 1a. The optical birefringence was

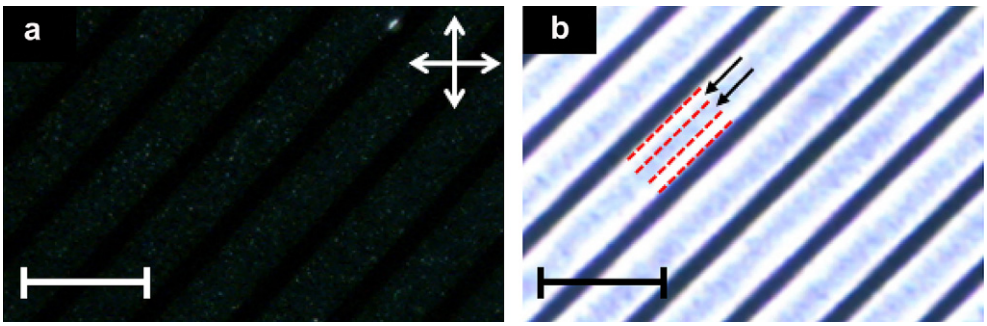


**Fig. 1.** Polarizing optical images of polymer-stabilized BP under crossed polarizers: (a) Off-state and (b) on-state with 6 V/μm of applied electric field at room temperature. The polymer-stabilized blue phase exhibits a dark state at zero field due to the intrinsic optical isotropy of the phase. The bright state is attributed to an optical birefringence induced by the *Kerr effect* under in-plane electric field. The nonuniform transmittance at an inter-electrodes area is indicated by the single-headed arrows in (b). The double-headed arrows represent a direction of polarizers and the scale bars correspond to 50 μm.

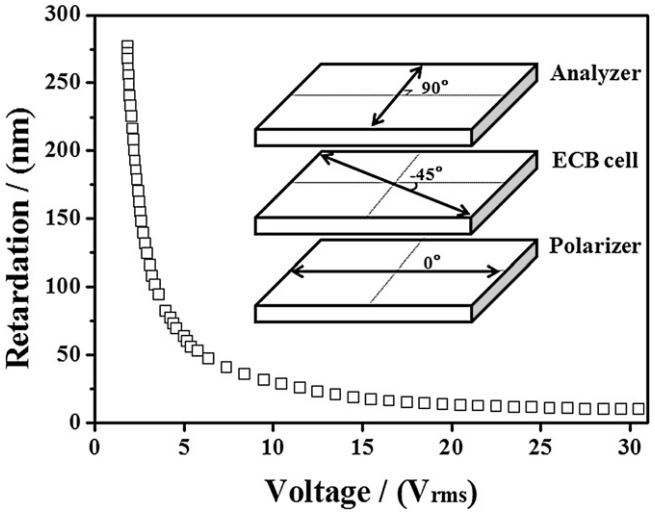


**Fig. 3.** Measured retardation values of the reference ECB cell as a function of applied voltage. The inset displays geometry of measurements where a uniaxial optic axis of ECB cell is aligned −45° to the polarizer. For the measurements, varied amplitude of square waveform voltage was applied at 60 Hz. The arrows on polarizer/analyzer represent transmission axes of linear polarizers.

induced by applying electric field due to a large *Kerr constant* of the LC composite originated from a local nematic order. As shown in Fig. 1b, the polarized optical image became bright by applying 6 V/μm of square waveform electric field at room temperature. The nonuniform brightness is clearly observed inter-electrode area as indicated by the arrows in Fig. 1b. As marked by broken lines, the near side of electrode edge is lighter that the central region of inter-electrode area. It will be beneficial if one can measure a local optical retardation in a micrometer scale and optimize optical transmittance to achieve a better performing device.

To examine a local retardation in a micrometer scale, we have conceived a new method by utilizing the reference LC cell with an electrically adjustable retardation value. As schematically demonstrated in Fig. 2, the reference ECB cell is placed after the *Kerr* (sample) cell at −45° and 90° with respect to the transmission axis of polarizer and the optic axis of the sample cell, respectively. In this geometry, the optical retardation originated from the sample is compensated by the retardation of a reference ECB cell since the slow axes of two uniaxial crystals are orthogonal to each other in the plane of the substrate. If the retardation from a sample is completely compensated by the reference cell, the net retardation becomes zero and consequently no transmitted light is observed. As the retardation value of a reference cell is electrically adjustable, multiple frames of POM images were taken with a designated local region while the retardation value of the ECB cell changes by a 2 nm step. The image processing software (i-Solution, *i*MTechnoloy) identified the darkest frame of the image for the designated area. Therefore, the retardation value of the sample is the same as that of a reference cell at the applied voltage for darkest specified region.

Fig. 3 displays measured retardation values of the reference ECB cell obtained by changing an applied voltage. The inset shows the geometry of measurements where the optic axis of the ECB cell is aligned −45° to the polarizer. For the measurements, varied amplitude of square waveform voltage was applied at 60 Hz. With the increase of applied voltage, the nematic director gradually aligns parallel to a vertical electric field and thus effective birefringence of the LC decreases, resulting in the decrease of retardation as seen in Fig. 3.

The local optical retardations of the cell with a polymer-stabilized BP were measured as a function of applied electric field by employing the process described above.

The inset of Fig. 4 shows a cross-sectional view of the bottom substrate and designated local areas for measured retardation are indicated by 1 (near electrode) and 2 (away from electrodes) with a 5 μm width and 15 μm length. The values shown in Fig. 4 are simply the same as a readout of the retardation values from the reference ECB cell that are adjusted, for a complete compensation of a local optical retardation from the *Kerr* cell, by changing applied voltage. As expected, except for a low field range, the electric field-induced retardation of the LC/polymer composite film exhibits approximately linear relation to the field strength for both specified regions. However the absolute values differ from each other. The induced optical retardation at near electrode edge (region 1) is relatively larger than that in the region 2 for the entire range of an applied field. These results are in corroboration with the POM

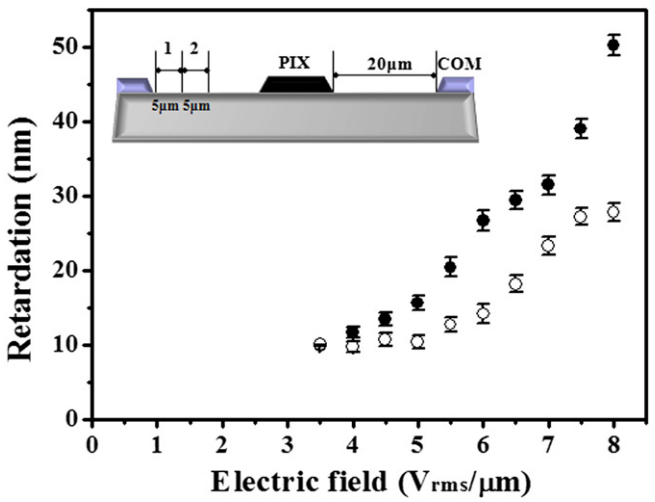


**Fig. 4.** Measured local retardation values of the *Kerr* cell as a function of applied electric field for different regions: Filled and empty circles for region 1 and 2, respectively. The inset shows a cross-sectional view of the bottom substrate and local areas for retardation measurement are indicated by 1 (near electrode) and 2 (away from electrodes) with 5 μm width.

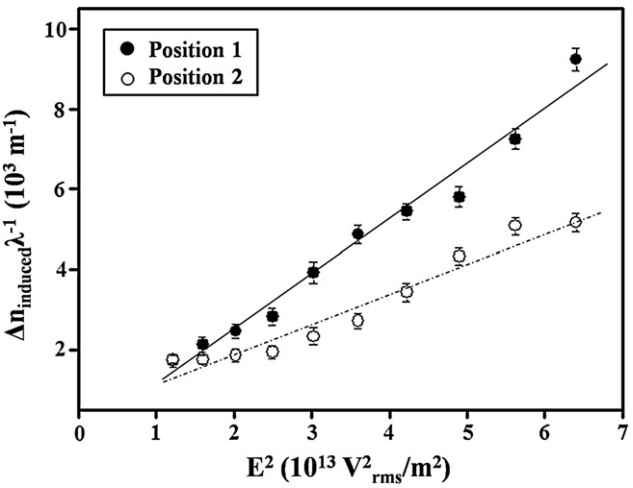


**Fig. 5.** Induced optical birefringence of the *Kerr* cell as a function of applied electric field at separate regions 1 (filled squares) and 2 (empty squares). The birefringence at both regions exhibits a linear relation with applied electric field. The slopes corresponding to the region 1 and 2 (i.e., *Kerr* constant of the polymer-stabilized LC composite) are slightly different each other. The solid lines are fitting lines.

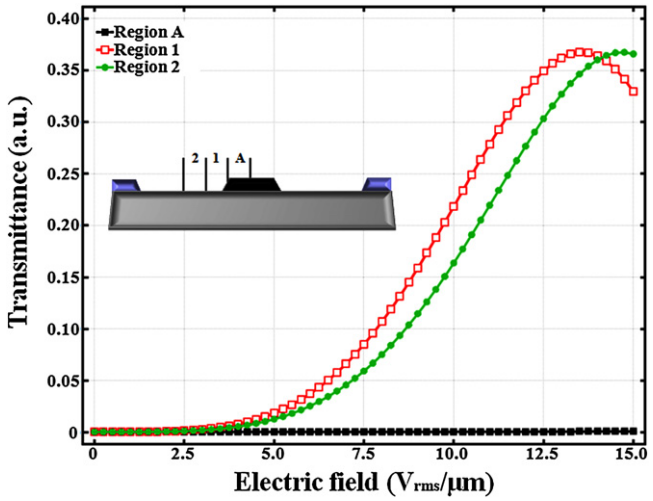


**Fig. 6.** Normalized optical transmittance as a function of applied electric field for different regions of inter-electrode area: Red squares for region 1 and green circles for region 2. The local regions used for calculations are presented in the inset. The filled squares correspond to transmittance from the area of pixel electrode marked by A in the inset.

image shown in Fig. 1b. This is presumably attributed to the nonuniform effective in-plane electric field in an inter-electrode area.

Fig. 5 presents induced optical birefringence of the *Kerr* cell as a function of applied electric field at separate regions 1 (filled squares) and 2 (empty squares). The birefringence at both regions linearly increases with applied electric field. The slopes in the region 1 and 2 (i.e., *Kerr constant* of the polymer-stabilized LC composite) are $2.25 \times 10^{-10}\,mV^{-2}$ and $1.56 \times 10^{-10}\,mV^{-2}$, respectively. The difference between two values is related to variations of effective applied electric field in between electrodes. If one measures *K* of the mixture in the in-plane field driven cell macroscopically without considering this effect, one would get kind of average value *K* between these two values, which might misinform about *K* of the mixture.

The normalized optical transmittance calculated as described in the experimental section and shown in Fig. 6 supports this assumption. The optical transmittance curves of both regions 1 (red squares) and 2 (green circles) plotted as a function of applied electric field exhibit a similar feature. The local designated regions used for calculations and presented in the inset were the same as those in the retardation measurements. The filled squares correspond to transmittance from the area of an opaque pixel electrode marked by A in the inset. By observing the slight shift of threshold field for the transition from the optically isotropic to birefringent state and considering a uniform LC/polymer composite film through the entire sample, it is reasonable to understand that the difference in retardation or birefringence is attributed to the nonuniform electric field in the area between electrodes.

## 4. Conclusions

The optical and electro-optical properties of a polymer-stabilized BP with in-plane electric filed have been studied. The local optical retardation in a microscopic scale was successfully determined by utilizing an *electrically controllable birefringence* LC cell and image processing software. By combining experimental results, we conclude that the observed nonuniform transmittance in the pixel area is attributed to the distribution of effective electric field created by interdigitated electrodes in the plane of substrate.

## Acknowledgement

This work was supported by WCU program through MEST (R31-2008-000-20029-0).

## References

[1] M. Oh-E, K. Kondo, Appl. Phys. Lett. 67 (1995) 3895.
[2] S.H. Lee, S.L. Lee, H.Y. Kim, Appl. Phys. Lett. 73 (1998) 2881.
[3] J.W. Park, Y.J. Ahn, J.H. Jung, S.H. Lee, Appl. Phys. Lett. 93 (2008) 081103.
[4] A. Takeda, S. Kataoka, T. Sasaki, H. Chida, H. Tsuda, K. Ohmuro, T. Sasabayashi, Y. Koike, K. Okamoto, SID Int. Symp. Digest Tech. Papers 29 (1998) 1077.
[5] K. Higashiguchi, K. Yasui, H. Kikuchi, J. Am. Chem. Soc. 130 (2008) 6327.
[6] W. He, G. Pan, Z. Yang, D. Zhao, G. Niu, W. Huang, X. Yuan, J. Guo, H. Cao, H. Yang, Adv. Mater. 21 (2009) 2050.
[7] Y. Tanabe, H. Furue, J. Hatano, Mater. Sci. Eng. B 120 (2005) 41.
[8] H. Kikuchi, M. Yokota, Y. Hisakado, H. Yang, T. Kajiyama, Nat. Mater. 1 (2002) 64.
[9] Y. Hisakado, H. Kikuchi, T. Nagamura, T. Kajiyama, Adv. Mater. 17 (2005) 96.
[10] Y. Haseba, H. Kikuchi, T. Nagamura, T. Kajiyama, Adv. Mater. 17 (2005) 2311.
[11] W. S-Choi, S. Yamamoto, Y. Haseba, H. Higuchi, H. Kikuchi, Appl. Phys. Lett. 92 (2008) 043119.
[12] T. Iwataa, K. Suzukia, H. Higuchic, H. Kikuchi, Liq. Cryst. 36 (2009) 947.
[13] Y. Haseba, H. Kikuchi, J. Soc. Inf. Display 14 (2006) 551.
[14] S.-W. Choi, S. Yamamoto, T. Iwata, H. Kikuchi, J. Phys. D: Appl. Phys. 42 (2009) 112002.
[15] J. Kerr, Philos. Mag. 50 (1875) 337.
[16] M. Kim, M.S. Kim, B.Y. Kang, M.K. Kim, S. Yoon, S.H. Lee, Z. Ge, L. Rao, S. Gauza, S.T. Wu, J. Phys. D: Appl. Phys. 42 (2009) 235502.
[17] H.H.H. Klausmann, S. Aratani, K. Kondo, J. Appl. Phys. 83 (1998) 15.